Available online at www.elixirpublishers.com (Elixir International Journal)

Pollution

Elixir Pollution 103 (2017) 45576-45583

ISSN: 2229-712X

Adsorption of Fe, Cu and Mn from Waste Waters of Al-Mohet Drain west El-minya by Iron Oxide Nanoparticles Coated by TiO_2 and Poly Vinyl Alcohol

Yasser A.M. Abdulhady[1] and Medhat Ibrahim [2]

[1]Water Treatment and Desalination Unit, Desert Research Center, Cairo, P.O.B 11753, Egypt.

[2] Spectroscopy Department, National Research Centre, 33 El-Bohouth St. 12622 Dokki, Giza, Egypt.

ARTICLE INFO

Article history:

Received: 15 November 2016;

Received in revised form:

27 January 2017;

Accepted: 6 February 2017;

Keywords

Iron,

Copper and manganese

Removal, wastewater treatment,

Magnetic nanoparticles,

Magnetic iron oxide coated TiO_2,

Poly vinyl alcohol,

Nitrate & phosphate removal,

Adsorption,

B3LYP/6-31G(d,p) .

ABSTRACT

Iron oxide nanoparticles with TiO_2 with PVA were synthesized by co- precipitation. Removal efficiency of iron, manganese and copper in wastewater by nano iron oxide after treatment was 91.10 %, 82.66 % and 94.03 %, respectively. Removal efficiency of Fe, Mn and Cu in synthesized solution after treatment was 91.42 %, 92.96 % and 90.81% respectively. Reduction percent of nitrate and phosphate in wastewater after treatment was observed to be 87.65 % and 91.07 % respectively. B3LYP/6-31G(d,p) indicated that PVA became more reactive as metals oxides are interacted with it as blending and complexing or both types of interaction.

1. Introduction

The morphology of the iron oxide particles depends on the competition between several processes like nucleation, growth, aggregation and adsorption of impurities.(1) Some of the synthesis techniques include chemical precipitation, sol-gel, hydrothermal, surfactant mediated-precipitation, emulsion-precipitation, micro-emulsion-precipitation, electro-deposition, and micro wave assisted hydrothermal technique. These oxides find applications as catalysts, sorbents, pigments, flocculants, coatings, gas sensors, ion exchangers and for lubrication.(2, 3, 4)

Iron oxide nano-composites have potential applications in areas such as magnetic recording, magnetic data storage devices, toners and inks for xerography, and magnetic resonance imaging, wastewater treatment, bio-separation, and medicine.(5, 6, 7, 8, 9, 10) Various approaches such as wet chemical,(11) template-directed,(12, 13) microemlusion,(14) thermal decomposition,(15) eposition method,(16) spray pyrolysis,(17) self-assembly,(18,19) physical have been extensively used for the synthesis of a wide variety of magnetic nanostructures including iron oxide, metal, metal alloys and core–shell and composites structures. Several chemical methods that are being used for the synthesis of magnetic nanostructures comprise of co-precipitation, and hydrothermal methods. Thermal decomposition and hydrothermal approaches provide better results (both in terms of size and morphology) in comparison with other synthetic routes. The precipitation technique is probably the simplest and most efficient chemical pathway to obtain iron oxide particles. Iron oxides (Fe OOH, Fe_3O_4 or γ-Fe_2O_3) are usually prepared by addition of alkali to iron salt solutions and keeping the suspensions for ageing. The main advantage of the precipitation process is that a large amount of nanoparticles can be synthesized. However, the control of particle size distribution is limited, because only kinetic factors are controlling the growth of the crystal.(20) Size control of mono dispersed particles must normally be performed during the very short nucleation period, because the final particle number is determined by the end of the nucleation and it does not change during particle growth. A wide variety of factors can be adjusted in the synthesis of iron oxide nanoparticles to control size, magnetic characteristics, or surface properties.(21,22). Molecular modeling at different level of theory could be applied to understand the reactivity of a given compounds.(23) Modeling could be utilized to design a novel structure for the removal of Pb from wastewater.(24)

Later on modeling could describe the mechanism at which TiO_2 in nanoscale could be utilized as photo catalytic agent.(25) The possible transport of pollutants from surface to ground water is described with molecular modeling and molecular spectroscopic methods.(26).

In this paper the preparation of nanocomposite materials with nano-sized is described. These different materials with different composition had a new cross linking structure that had new structure in nano-sized diameter. The iron oxide was reprehensive as a core and TiO_2 coated the outer shell of iron oxide. The presence of PVA gave more strength and increase functional activity for nanoparticles.

Tele: 002 01016941598

E-mail address: yasser_vip6@hotmail.com

The characterization analysis by different instruments showed that iron oxide coated by TiO_2 was in the nano-sized range. The mechanism of interaction is described with molecular modeling at B3LYP/6-31G(d,p) level of theory.

2. Materials and Methods

2.1. Chemicals and reagents

All chemical materials used in this study were provided from Merck and Sigma Aldrich Companies.

2.2. Experimental Procedure

2.2.1. Sol-gel route

The sol-gel synthesized TiO_2 was obtained from Titanium (IV) isopropoxide (TTIP) was dissolved in absolute ethanol and distilled water was added to the solution in terms of a molar ratio of Ti: H_2O=1:4. Citric acid was used to adjust the pH and for restrain the hydrolysis process of the solution. The solution was vigorously stirred for different reaction time in order to form sols. After aging for 12 hrs, the sols were transformed into gels. In order to obtain nanoparticles, the gels were dried under 100^{o}C for 5 hr to evaporate water and organic material to the maximum extent. Then the dry gel was sintered at 450^{o}C for 3 hrs were subsequently carried out to obtain desired TiO_2 nano-crystalline.

2.3. Synthesis of Iron oxide NPs with poly vinyl alcohol.

2.3.1. Sample preparation

The reagents were used for the synthesis were ferric chloride hexa-hydrate ($FeCl_3 \cdot 6H_2O$), ferrous chloride tetra-hydrate ($FeCl_2 \cdot 4H_2O$), propylene glycol (CH_3CH (OH) CH_2 (OH), sodium hydroxide (NaOH), poly vinyl alcohol and ammonium hydroxide (NH_4OH, 26% of ammonia). It was synthesized by the co-precipitation method. A Certain weight of ferric chloride was added to ferrous chloride molar ratio of Fe^{3+}/Fe^{2+}=(1:2) and 150ml of (NH_4OH, 26% of ammonia) with 300 ml of de-ionized water in a 500 ml flask. Subsequently, Afterwards, and then the resultants were aged for 20 min before being separated. The formation of magnetic nano-iron particles:

$$Fe^{2+} + 2Fe^{3+} + 8NH_3 \cdot H_2O \longrightarrow Fe_3O_4\downarrow + 8NH + 4H_2O$$

2.3.2. Sample characterization

FT-IR spectra were measured in a transmission mode on a spectrophotometer (PerkinElmer Spectrum Version 10.03.09) Spectrum Two Detector $LiTa0_3$ was used for separating the solid and liquid during the preparation samples. The samples were pressed pellets of a mixture of the powder with KBr. The micrographs of prepared particles were obtained using a Scanning Electron Microscope using SEM Model Quanta 250 FEG (Field Emission Gun). The XRD pattern of TiO_2 and MNPs was obtained using a X-ray diffractometer Schimadzu model: A PAN analytical X-rays diffraction equipment model Xpert PRO with secondary monochromator, Cu-radiation (λ=1.54A^0) at 50k.v.,40 M.A and scanning speed 0.02^o /sec. Magnetic properties of the particles were assessed with a vibrating-sample magnetometer (VSM, Homade 2 tesla). A magnet (Φ 17.5×20 mm, 5500 O e) was utilized for the collection of magnetic particles**.** Basing on the results of measurements, coercivity, remanence and saturation of samples have been determined, from each powder sample a certain amount of sample has been portioned out, put into another container and weighted. The VSM measurements have been performed on every sample.

2.3.3. Examine adsorbents efficiency

Batch adsorption studies were performed by mixing MNPs with 50 ml of the synthesized wastewater in a flask. For pH adjustment we used standard 0.1M HCl and 0.1M NaOH solutions. Put the solution mixture of MNPs with wastewater solution in sonicator for different time. After adsorption reached equilibrium, the adsorbent was conveniently separated via an external magnetic field and the solution was collected for metal concentration measurements. MNPs were washed thoroughly with deionized water to neutrality. The concentrations of metal ions were measured by a plasma-atomic emission spectrometer (ICP-AMS, Optima 3000XL, PerkinElmer) in accordance with the Standard Method. In order to obtain reproducible experimental results, the adsorption experiments were carried out at least 3 times.

2.3.4. Laboratory analyses

The analyses include the determination of EC, TDS, pH. The minor, trace and soluble heavy metals and non metals are total nitrogen, NO^{3-}, PO_4^3, B^{3+}, Al^{3+}, Fe^{3+}, Mn^{2+}, Co^{2+}, Cu^{2+}, Ni^{2+}, Cr^{3+}, Cd^{2+}, Pb^{2+}, and Zn^2.

2.3.5. Computational Details

The studied structures were subjected to optimization with B3LYP using 6-31g(d,p) basis set[27,28,29] implemented in Gaussian 09[30] program at Spectroscopy Department, National Research centre, Egypt. The total dipole moment and band gap energy were calculated at the same level of theory.

3. RESULTS and DISSCUSION

3.1. Mechanism of iron nanocomposite coated by TiO_2 in presence PVA.

$Fe(OH)_2$ and $Fe(OH)_3$ formed at pH > 8 by the hydroxylation of the ferrous and ferric ions. Black precipitation is formed immediately with addition of NH_4OH with drop wise of NaOH. The $FeCl_3$ reacts with NH_4OH and forms FeOOH, which, upon heating, further produce into Fe^{2+} and OH^- ions, which consequently assists in the development of Fe_2O_3 ions according to the chemical reactions. The iron oxide nanoparticles formed in solution with addition of poly vinyl alcohol the polymerization chain increased and the morphology of iron oxide nanoparticles is changed and have hydroxyl function group with more reduction efficiency occurred. The addition of TiO_2 in reaction to form nano-composite coated the iron oxide nanoparticles. This composite had more specific functional group and more free electrons in dispersion solution that can increase the reduction percent of removal heavy metals.

Step 1: $3\ FeO + 2O_2 \longrightarrow Fe_3O_4$

Step 2: $4\ Fe_3O_4 + O_2 \longrightarrow 6\ \gamma\text{-}Fe_2O_3$

Step3: $4\ Fe_3O_4 + O_2 + 2\ H_2O \longrightarrow 4\ \gamma\text{-}Fe_2O_3 + 4\ FeOOH$

3.2 Characterization of the adsorbents

3.2.1. Infrared Spectroscopy (FT-IR)

Figure (1) Absorption peaks at 530 cm−1 indicated to the Fe–O vibration related to the magnetite and two absorption peaks at 2,924 and 2,854 cm−1 were attributed to the asymmetric CH_2 stretching and the symmetric CH_2 stretching, respectively.[31] The bands due to C–O stretching mode were merged in the very broad envelope centered on 1168 and 1009 cm−1 arising from C–O, C–O–C stretches and C–O–H bends vibrations of iron oxide nanoparticles in poly vinyl alcohol. The aliphatic C–H stretching, in 1313 and 1404 cm−1 were due to C–H bending vibrations. The broad band at 520-650 cm–1 is likely due to the vibration of the Ti–O bonds in the TiO_2 lattice.[32] The broad peak in 407 cm^{-1} related to iron oxide NPs banding with TiO_2. The IR band at 1643 cm^{-1} is close to the position of H_2O bending vibrations.

The IR band at 3455 cm^{-1} can be assigned to the stretching modes of surface H_2O molecules or to an envelope of hydrogen-bonded surface OH groups.

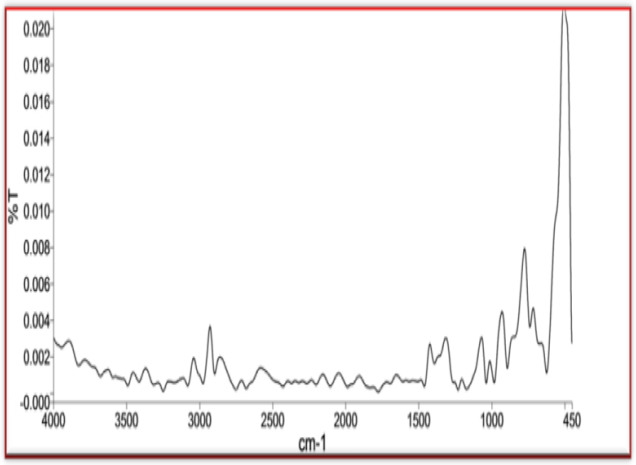

Fig 1. FTIR spectra of the iron oxide nanoparticles composite with TiO_2 and Poly Vinyl Alcohol

3.2.2. X-Ray Diffraction Analysis (XRD)

Figure (2) showed peaks at 2θ of 15.8°, 22.4°,29.2°, 32.3°, 41.9°, 52.5° corresponding to the diffractions of crystal faces poly vinyl alcohol, TiO_2 anatase, hematite and magnetite spinal structure. The positions and relative intensities of the reflection peak of Fe_3O_4 and Fe_2O_3 MNPs agree with the XRD diffraction peaks of standard Fe_2O_3 samples.[33] Sharp peaks showed that Fe_3O_4 and Fe_2O_3 nanoparticles have well crystallized structure.

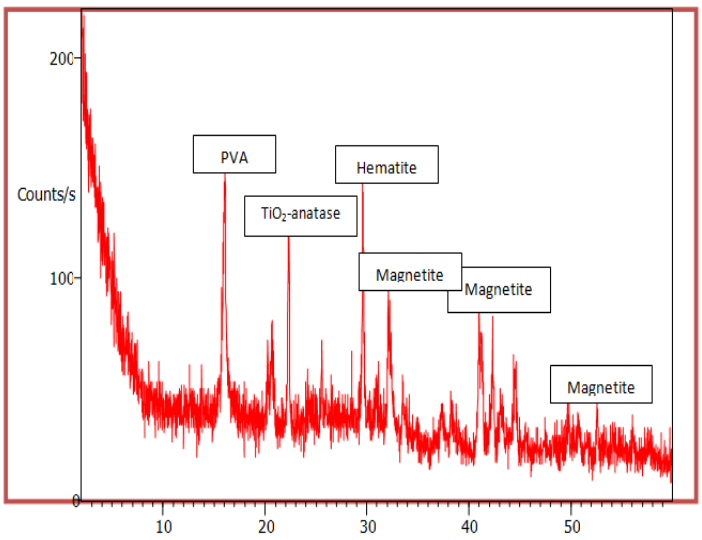

Fig 2. XRD spectra of the iron oxide nanoparticles composite with TiO_2 and Poly Vinyl Alcohol.

Mineral Name	Chemical Formula	Semi-Quant [%]
Titanium oxide	TiO_2	10
Poly vinyl alcohol	PVA	15
Magnetite	Fe_3O_4	55
Hematite	Fe_2O_3	20

Fig 2. XRD spectra of the iron oxide nanoparticles composite with TiO_2 and Poly Vinyl Alcohol

3.2.3. Scanning Electron Micrograph (SEM)

Figure (3) showed the SEM images of nano iron oxide with TiO_2 and Poly Vinyl Alcohol, which confirms that the cubic and spherical shape of iron oxide nanoparticles of magnetite and hematite merged with the cross linking of PVA polymer and coated with TiO_2 in bending structure so that the SEM photo showed the homogenous surface and distribution with smoothly surface and homogenous pores and size.

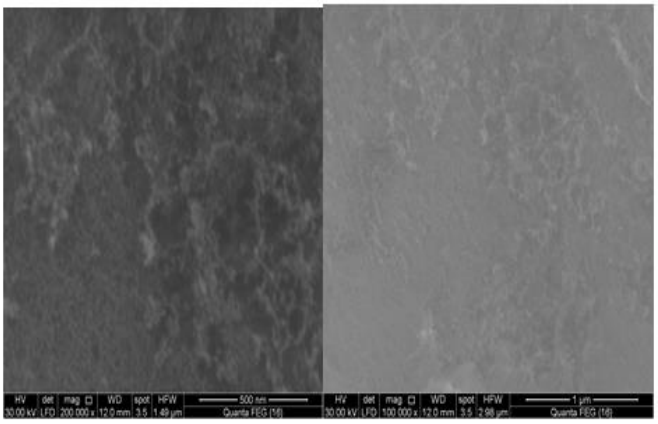

Fig3. Scanning Microscope (SEM) for iron oxide nanocomposite with TiO_2 and Poly Vinyl Alcohol

3.2.4. Vibrating Sample Magnetometer (VSM)

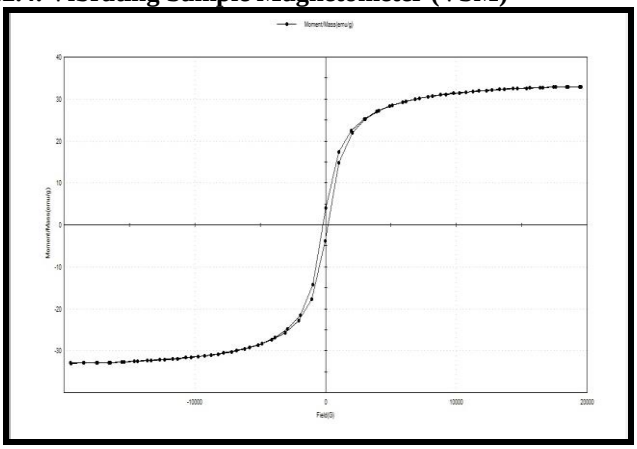

Fig 4. Magnetization curves of for iron oxide nanocomposite with TiO_2 and Poly Vinyl Alcohol.

The magnetization curves measured at room temperature for iron oxide nanoparticles coated with TiO_2 in presence of poly vinyl alcohol are showed in Figure 4. The low hysteresis in the magnetization for sample showed that produced nanoparticles had paramagnetic strength.[34] The saturation magnetization value was 81.40 emu g^{-1} for Fe_3O_4. The high saturation magnetization of pure Fe_3O_4 indicated the good crystal structure. The saturation magnetization values of TiO_2 coated Fe_3O_4 was smaller than the value for the pure magnetite nanoparticles, therefore the saturation magnetization was reduced after coating of TiO_2 onto the surface of Fe_3O_4 and Fe_2O_3 MNPs. The figure indicated that magnetite and hematite nanoparticles were merged in the composite particles, which exhibited no remanence effect from the hysteresis loops at applied magnetic field.

3.3. Effect of iron nanocomposite coated by TiO_2 in presence PVA on contaminated wastewater

3.3.1. Removal of iron, copper and manganese metals by iron magnetic nanocomposite.

Pollutants analyses level in water (inorganic, biological, and organic contaminations) was discussed on the basis of determination with regard to the recommended level of Egyptian guideline (1995), Egyptian standards (1995), Higher committee for water (1995) and WHO (1996). Table (1) showed that the raise level of iron, copper and manganese metals were in permissible standard level. Before treatment the concentration of iron in wastewater was 13.72 ppm as shown in table (1) and it decreased to 1.22 ppm as shown in table (2) after treatment with iron nanocomposite coated TiO_2 in presence of PVA. This inhibition indicated that the adsorption efficiency of prepared nanocomposite was(91.10%)

as shown in table (3) and the nano-composite had a nanosized shape with large surface area at optimal condition done. Concentration of copper after treatment decreased to 1.56 ppm as shown in table (2) from 26.16 ppm before treatment as shown in table (1) with reduction percent(94.03) table (3). The concentration of manganese in wastewater before treatment by nano-composite was 9.17 ppm and after treatment reached to 1.59 ppm with reduction percent 82.99 % table (3).

3.3.2. Removal of nitrate and phosphates by magnetic iron nanocomposite coated by TiO_2 in presence PVA

Table (4) showed that the ability of magnetic nanocomposite iron / TiO_2 in presence PVA for removal of nitrate group and nitrate derivatives. The adsorption efficiency (mean reduction percent) of adsorbed nitrate on nanocomposite particles was 87.65 %. The reaction mechanism of adsorption depends on the formation of weak interaction between hydroxyl group and lone pair of electrons on nitrogen atom.

3.3.3. Removal of Phosphate content by magnetic Iron/TiO_2 nanocomposite

In table (4), the reduction percent of phosphate group adsorbed on nanocomposite particles the mean reduction percent was 91.07 %. The increase of reduction percent caused by the increasing of adsorption and desorption of phosphate group on nanocomposite particles and largest molecular weight of phosphate group.

Table 4. Reduction percent of nitrate and phosphate by Nanocomposite before and after treatment of polluted waters.

Serial	NO_3-N ppm P.L: 10 to 50 mg/l			PO_4-P ppm P.L: 10 to 30 mg/l		
	B.T	A.T	R %	B.T	A.T	R %
A	170.25	22.57	86.74	34.98	2.70	92.28
B	120.38	12.36	89.73	44.98	4.90	89.10
C	254.70	30.41	88.06	60.01	5.30	91.16
S.S	40.56	5.65	86.07	60.29	4.96	91.77

S.S: Synthesized solution; B.T: Before treatment; A.T: After treatment; R: Reduction%; P.L: permissible limit

Table 1. Analysis of heavy metals in ppm before treatment.

Parameter	Permissible limit	A (Cu)2	B (Fe)29	C (Mn)42
	----	8.64 PH	6.20 PH	7.86 PH
Aluminum, mg/l	<0.2	0.19	0.1394	0.02
Boron, mg/l	<0.5	0.487	0.328	0.175
Cadmium, mg/l	<0.005	0.004	<0.0006	<0.0006
Cobalt, mg/l	<0.05	0.00932	<0.001	<0.001
Chromium, mg/l	<0.05	0.046	<0.02	<0.02
Copper, mg/l	<0. 5	26.16	<0.009	<0.009
Iron, mg/l	<0.3	0.2701	13.72	0.03
Manganese, mg/l	<0.5	0.0646	0.2041	9.173
Molybdenum, mg/l	<0.01	0.0032	0.001	0.0034
Nickel, mg/l	<0.1	0.05	<0.003	<0.002
Lead, mg/l	<0.05	0.0323	0.0152	0.0169
Vanadium, mg/l	<0.01	0.004	<0.01	<0.01
Zinc, mg/l	<5	4.413	0.0145	<0.002

Table 2. Analysis of heavy metals in ppm after treatment.

Parameter	Permissible limit	A (Cu)2	B (Fe)29	C (Mn)42
	----	8.64 PH	6.20 PH	7.86 PH
Aluminum, mg/l	<0.2	0.413	0.1394	0.02
Boron, mg/l	<0.5	0.487	0.328	0.175
Cadmium, mg/l	<0.005	0.004	<0.0006	<0.0006
Cobalt, mg/l	<0.05	0.00932	<0.001	<0.001
Chromium, mg/l	<0.05	0.046	<0.02	<0.02
Copper, mg/l	<0. 5	1.56	0.0	0.0
Iron, mg/l	<0.3	0.0	1.22	0.0
Manganese, mg/l	<0.5	0.0	0.0	1.59
Molybdenum, mg/l	<0.01	0.0032	0.001	0.0034
Nickel, mg/l	<0.1	0.05	<0.003	<0.002
Lead, mg/l	<0.05	0.0323	0.0152	0.0169
Vanadium, mg/l	<0.01	0.004	<0.01	<0.01
Zinc, mg/l	<5	4.413	0.0145	<0.002

Table3. Reduction percent of copper & Iron and manganese before and after treatment by iron nano-composite coated by TiO_2 in presence PVA of polluted waters.

Serial	Copper/ ppm			Iron/ ppm			Manganese/ ppm		
	B.T	A.T	R %	B.T	A.T	R %	B.T	A.T	R %
A	26.16	1.56	94.03	0.27	0.0	100	0.204	0.0	100
B	<0.009	0.0	100	13.72	1.22	91.10	0.06	0.0	100
C	<0.009	0.0	100	0.03	0.0	100	9.173	1.59	82.66
S. S	32.89	3.02	90.81	64.58	5.54	91.42	49.32	3.47	92.96

S.S: Synthesized solution; B.T: Before treatment; A.T: After treatment; R: Reduction%.

Table 5. Effect of different conditions with iron concentration.

Iron ppm R %	N. Conc. g/50ml A.T	Iron ppm R %	N. Conc. g/50ml A.T
68.51	20.33	68.51	20.33
75.82	15.61	75.82	15.61
83.36	10.74	83.36	10.74
80.58	12.54	80.58	12.54

R. Time Min.	Iron ppm		
	R %	R %	R %
5	75.99	75.99	75.99
10	86.40	86.40	86.40
15	86.37	86.37	86.37
20	86.20	86.20	86.20

PH	Iron ppm		
	B.T	A.T	R %
5	64.58	26.54	58.90
6	64.58	13.65	78.86
7	64.58	11.50	82.19
8	64.58	16.71	74.12

R. Temp.°C	Iron ppm		
	B.T	A.T	R %
20	64.58	20.43	68.36
25	64.58	11.22	82.62
30	64.58	16.87	73.87
35	64.58	27.98	56.67

B.T: Before treatment; A.T: After treatment; R: Reduction%
Optimal condition: Nanoparticles conc. 0.05g/50ml sonicated for 10 min. at PH 7 and 25 °C

Table 6. Effect of different conditions with copper concentration.

N. Conc. g/50ml	Copper ppm		
	B.T	A.T	R %
0.015	32.89	5.64	83.39
0.025	32.89	4.32	86.86
0.05	32.89	2.89	91.21
0.10	32.89	3.89	88.17

R. Time Min.	Copper ppm		
	B.T	A.T	R %
5	32.89	10.73	67.37
15	32.89	7.92	75.91
25	32.89	1.46	95.56
40	32.89	3.50	89.35

pH	Copper ppm		
	B.T	A.T	R %
5	32.89	9.67	70.59
6	32.89	4.65	85.86
7	32.89	1.82	94.46
8	32.89	6.21	81.11

R. Temp. °C	Copper ppm		
	B.T	A.T	R %
20	32.89	8.76	73.36
25	32.89	1.21	96.32
30	32.89	1.86	94.34
35	32.89	5.54	83.15

B.T: Before treatment; A.T: After treatment; R: Reduction%

Optimal condition: Nanoparticles conc. 0.05 g/50ml sonicated for 10 min. at PH 7 and 25 ^{0}C

Table 7. Effect of different conditions with Manganese concentration.

N. Conc. g/50ml	Manganese ppm		
	B.T	A.T	R %
0.015	49.32	9.74	80.25
0.025	49.32	5.06	89.74
0.05	49.32	1.58	96.79
0.10	49.32	2.49	94.95

R. Time (Min.)	Manganese ppm		
	B.T	A.T	R %
5	49.32	10.71	78.28
15	49.32	3.66	92.57
25	49.32	1.12	97.72
40	49.32	2.18	95.57

pH	Manganese ppm		
	B.T	A.T	R %
5	49.32	10.26	79.19
6	49.32	4.91	90.04
7	49.32	1.07	97.83
8	49.32	2.98	93.95

R. Temp. °C	Manganese ppm		
	B.T	A.T	R %
20	49.32	4.21	91.46
25	49.32	1.65	96.65
30	49.32	1.97	96.00
35	49.32	3.80	92.29

B.T: Before treatment; A.T: After treatment; R: Reduction%
Optimal condition: Nanoparticles conc. 0.05g/50ml sonicated for10 min. at PH 7 and 25 ^{0}C

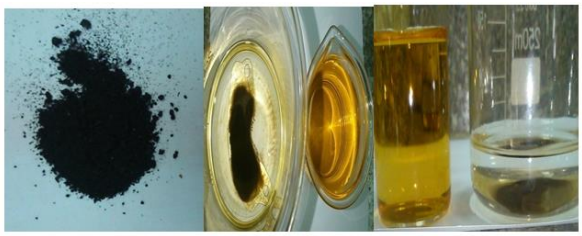

3.4. Building the Model Molecules

For molecular modeling study the first step is to build the model molecules. PVA is designed as indicated in figure (5). TiO_2 is supposed to interact with PVA through interaction with hydrogen bonding as shown in figure (6). There are two mechanisms for interaction the first one is complex formation, the second one is blending through weak hydrogen bonding.

The same is tried for Fe_3O_4 as indicated in figure (7). Then PVA is supposed to interact with both TiO_2 and Fe_3O_4 as shown in figure 8 also through complexation and blending. The final model is designed as PVA is supposed to interact with TiO_2 and Fe_3O_4 through both complexation and blending together as shown in figure (8).

The reactivity of a given chemical structure is expressed in terms two important physical quantities the total dipole moment and HOMO/LUMO band gap energy. It is stated that, the higher the dipole moment the higher the reactivity of the given structure. While lower band gap energy reflects the increasing in reactivity.[37]

As shown in figures (5) to (8) and table (8), PVA is calculated at B3LYP /6-31g(d,p). PVA is blended with TiO_2 and Fe_3O_4 separately then together.

The polymer is then assumed to make both types of interactions as blend and complex together.The reactivity is tested for each configuration with total dipole moment and bang gap energy as shown in table (8). The total dipole moment for PVA is 5.016 Debye, the band gap energy is 7.144 eV. As it complexes with TiO_2 its dipole moment is increasing up to 14.355 Debeye while band gap energy is decreased to 2.817 eV. Complexeing with Fe_3O_4 not affecting the total dipole moment (4.903 eV)while the band gap energy is further decreased down to 0.934 eV. Complexing with both metal oxides show both increase in total dipole moment and decrease in band gap energy.

The interaction with the same structures tried as adsorbed (blend) state show nearly the same behavior as for the case of complex between PVA and metal oxides.

The last case both type of interactions are tried simultaneously blend and complexation, results indicate that if the metals are interaction through both schemes blending and complexing the reactivity became more as total dipole moment became 20.532 Debye while the band gap energy is 0.304 eV.

Modeling results show that whenever the type or scheme of coordination between metals oxide and PVA the reactivity increased according to the huge surface area and the process of redistribution in the charge which increases the total dipole moment and decrees the HOMO/LUMO band gap energy. These data dedicate the studied blend and/or complexes for many applications such as environmental applications due to its ability to interact with the surrounding molecules regarding their charges and surface area.

4. Conclusion

The aim of this work was to remove heavy (toxic) metals by using magnetic iron oxide nanoparticles coated with TiO_2 in presence of poly vinyl alcohol. The removal efficiency percent of iron, copper and manganese in contaminated water of kotchner drain was 91.10 %, 94.03 % and 82.66 % respectively. Mean Reduction percent of nitrate and phosphate in wastewater after treatment was 87.65 % and 91.07 % respectively. These results was considered as good yield to treat wastewater of kotchner drain and this technology could be used to reuse polluted water and used as irrigation water in Egypt. The characterization analysis by different instruments showed that iron oxide coated by TiO_2 was in the nano-sized range. Presence of PVA gave the nano particles more dispersion efficiency. The saturation magnetization of the iron nano-composite was proportional to the particle size. The adsorption process is a function of pH, reaction time, adsorbent concentration and temperature. It is recommended to design a prototype to apply this technique in industry.

Molecular modeling at B3LYP/6-31G(d,p) level of theory indicate that the studied metal oxides enhances the reactivity of PVA for any scheme of interaction blend and/or complex.

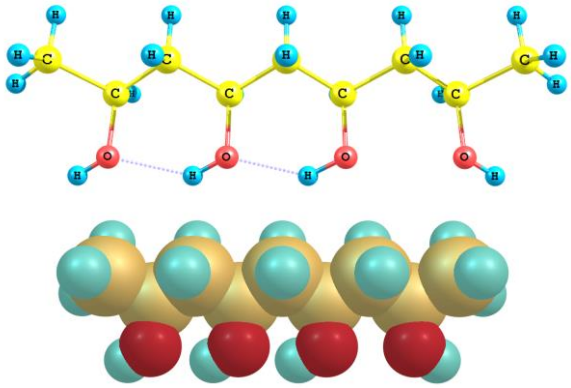

Fig 5. The model structure of the Poly(vinyl alcohol PVA.

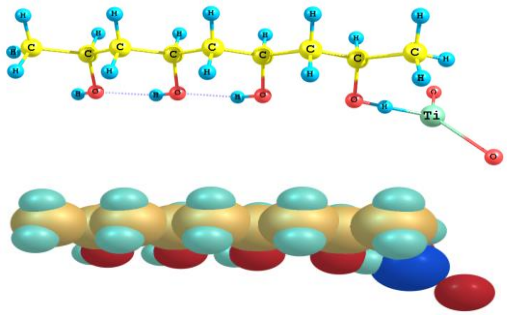

Fig 6. The model structure of the Poly(vinyl alcohol PVA whereas TiO_2 is interacted with PVA through hydrogen bonding.

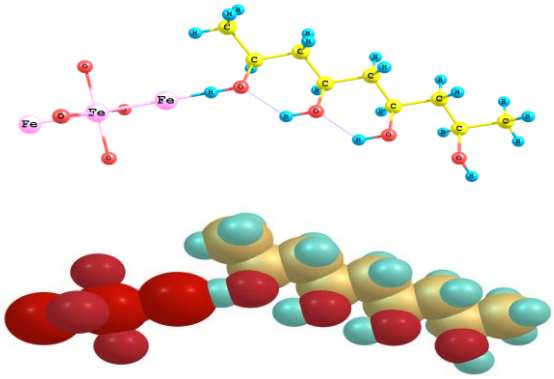

Fig 7. The model structure of the Poly(vinyl alcohol PVA whereas Fe_3O_4 is interacted with PVA through hydrogen bonding.

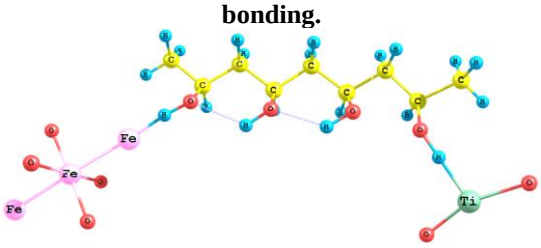

Table 8. Complex and blend mechanizing of individual or iron nano-composites.

	PVA	PVA-TiO_2	PVA-Fe_3O_4	PVA-TiO_2- Fe_3O_4
Complex				
Total dipole moment , Debye	5.016	14.355	4.903	10.374
Band gap energy, eV	7.144	2.817	0.934	1.050
Blend				
Total dipole moment , Debye	5.016	12.515	4.822	11.833
Band gap energy, eV	7.144	2.687	0.968	0.875
Complex and Blend				
Total dipole moment , Debye	5.016	20.207	9.579	20.532
Band gap energy, eV	7.144	1.873	0.527	0.304

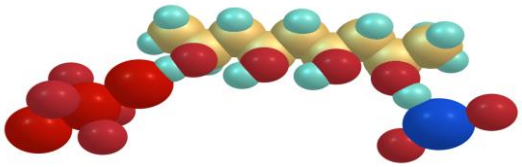

Fig 8. The model structure of the Polyvinyl alcohol PVA whereas TiO_2 and Fe_3O_4 are interacted with PVA through two hydrogen bondings.

References

[1]R.M. Cornell, and U. Schwertmann, Iron oxides. 2nd Edn., Wiley-VCH Verlagsgesellschaft Weinheim, 2003.

[2]T. Miyata, Y. Ishino, and T. Hirashima, "Catalytic Reduction of Aromatic Nitro Compounds with Hydrazine Hydrate in the Presence of Iron (III) Oxide Hydroxide," Synthesis, vol. 11, 1978, pp. 834-835.

[3]I.S. Lim, G.E. Jang, C.K. Kim, and D.H. Yoon, "Fabrication and Gas Sensing Characteristics of Pure and Pt-doped γ-Fe_2O_3 Thin Film," Sensor Actuat. B-Chem., Vol. 77, No.1-2, 2001, pp. 215-220.

[4]C.R. Catlow, J. Corish, J. Hennesy and W.C. Mackrod, "Theoretical Calculation of the Textures and Ion Transport in Alpha- Fe_20_3 and Alpha-Cr_20_3," J. Am. Ceram. Soc., Vol.71, 1988, pp. 42-49.

[5]K. Raj and R. Moskovitz, "Commercial Applications of Ferrofluids," J. Magn. Magn. Mater., Vol. 85, 1990, pp. 233-245.

[6]B.R. Pieters, R.A. Williams, C. Webb and R.A. Williams, "In: Colloid and Surface Engineering Applications in the Process Industries, Butterworth-Heinemann, Oxford, 1992, pp. 248.

[7]F. Ziolo Ronald, P. Giannelis Emmanuel, A. Weinstein Bernard, P. O'Horo Michael, N. Ganguly Bishwanath, V. Mehrotra, W. Russell Michael and R. Huffman Donald, "Matrix-mediated Synthesis of Nanocrystalline γ-Fe_2O_3: A New Optically Transparent Magnetic Material," Science, vol. 257(5067), 1992, pp. 219-223.

[8]I. Safarík, "Removal of Organic Polycyclic Compounds from Water Solutions with a Magnetic Chitosan Based Sorbent Bearing Copper Phthalocyanine Dye," Water Res., vol. 29, 1995, pp.101-105.

[9]U. Häfeli, W. Schütt, J. Teller, and M. Zborowski, Scientific and Clinical Applications of Magnetic Carriers. Plenum Press, New York, 1997.

[10]A. Denizli and R. Say, "Preparation of Magnetic Dye Affinity Adsorbent and its Use in the Removal of Aluminium Ions," J. Biomater. Sci. Polym. Edn., vol.12, 2001, pp.1059-1073.

[11]Z. Zhong, M. Lin , V. Ng, G.X. Boon Ng , Y. Foo , and A. Gedanken, "A Versatile Wet-chemical Method for Synthesis of One-dimensional Ferric and Other Transition Metal Oxides," Chemistry of materials, vol. 18, no. 25, 2006, pp. 6031-6036.

[12]F. Jiao, J.C. Jumas, M. Womes, A. V. Chadwick, A. Harrison, and P.G. Bruce, "Synthesis of Ordered Mesoporous Fe3O4 and γ-Fe2O3 with Crystalline Walls Using Post-template Reduction/Oxidation," J. Am. Chem. Soc., vol. 128, no. 39, 2006, pp. 12905-12909.

[13]Du, N., et al., "Selective Synthesis of Fe2O3 and Fe3O4 Nanowires via a Single Precursor: a General Method for Metal Oxide Nanowires," Nanoscale Res. Lett., vol. 5, no. 8, 2010, pp. 1295-1300.

[14]Wang, G., et al., "The Synthesis of Magnetic and Fluorescent Bi-functional Silica Composite Nanoparticles via Reverse Microemulsion Method," J. Fluoresc., vol. 19, no. 6, 2009, pp. 939-946.

[15]S. Sun, H. Zeng, D.B. Robinson, S. Raoux, P.M. Rice, S.X. Wang and G. Li, "Monodisperse MFe_2O_4 (M = Fe,. Co, Mn) Nanoparticles. J. Am. Chem. Soc. vol. 126, 2004, pp. 273-279.

[16]Q. Guo, X. Teng , S. Rahman , and H. Yang "Patterned Langmuir-Blodgett Films of Monodisperse Nanoparticles of Iron Oxide Using Soft Lithography. J. Am. Chem. Soc., vol. 125, no. 3, 2003, pp. 630-631.

[17]D. Dosev, M. Nichkova, R.K. Dumas, S.J. Gee, B.D. Hammock, K. Liu and I.M. Kennedy, "Magnetic/Luminescent Core/Shell Particles Synthesized by Spray Pyrolysis and Their Application in Immunoassays with Internal Standard," Nanotechnology, vol. 18, no. 5, 2007, pp. 055102.

[18]L.S. Zhong, J.S. Hu, H.P. Liang, A.M. Cao, W.G. Song and L.J. Wan, "Self-Assembled 3D Flowerlike Iron Oxide Nanostructures and their Application in Water Treatment," Adv. Mater., vol. 18, no. 18, 2006, pp. 2426-2431.

[19]V. Polshettiwar, B. Baruwati, and R.S. Varma, "Self-assembly of Metal Oxides into Three-dimensional Nanostructures: Synthesis and Application in Catalysis," ACS Nano, vol. 3, no. 3, 2009, pp. 728-736.

[20]P. Tartaj, M.P. Morales, S. Veintemillas-Verdaguer, T. Gonzalez-Carreno, and C.J. Serna, Synthesis, Properties and Biomedical Applications of Magnetic Nanoparticles. Handbook of Magnetic Materials; Elsevier: Amsterdam, the Netherlands. 2006.

[21]R. Weissleder, Monocrystalline Iron Oxide Particles for Studying Biological Tissues. U.S. Patent No. 5,492,814, 1996.

[22]H. Pardoe, W .Chua-anusorn, T.G.St. Pierre and J. Dobson, "Structural and Magnetic Properties of Nanoscale Iron Oxide Particles Synthesized in the Presence of Dextran or Polyvinyl Alcohol," J. Magn.Magn. Mater., vol. 225, no. 1-2, 2001, pp. 41-46.

[23]M. Ibrahim and A-A. Mahmoud, "Computational Notes on the Reactivity of some Functional Groups", J. Comput. Theor. Nanosci., vol. 6, 2009, pp. 1523–1526.

[24]N.S. Ammar, H. Elhaes, H.S. Ibrahim, W. El-hotaby and M.A. Ibrahim, "A Novel Structure for Removal of Pollutants from Wastewater", Spectrochimica Acta Part A., vol. 121C, 2014, pp. 216-223.

[25]A. Okasha, F. Gomaa, H. Elhaes, M. Morsy, S. El-Khodary, A. Fakhry and M. Ibrahim, "Spectroscopic Analyses of the Photocatalytic Behavior of Nano Titanium Dioxide," Spectrochim. Acta A., vol. 136, 2015, 504-509.

[26]A. Fakhry, O. Osman, H. Ezzat and M. Ibrahim, "Spectroscopic Analyses of Soil Samples Outside Nile Delta of Egypt," Spectrochim. Acta A., vol. 168, 2016, pp. 244–252

[27]C. Lee, W. Yang and R.G. Parr, " Development of the Colle-Salvetti Correlation-energy Formula into a Functional of the Electron Density," Phys. Rev. B., vol. 37, 1988, pp. 785.

[28] A.D. Becke, " A new mixing of Hartree–Fock and Local Density-functional Theories ", J. Chem. Phys., vol. 98, no. 2, 1993, pp. 1372.

[29]J.P. Perdew, M. Ernzerhof and K. Burke, " Rationale for Mixing Exact Exchange with Density Functional Approximations ", J. Chem. Phys., vol. 105, no. 22, 1996, pp. 9982.

[30]Gaussian 09; Revision C.01; MJ Frisch; GW Trucks; HB Schlegel; GE Scuseria; MA Robb; JR Cheeseman; G Scalmani; V Barone; B Mennucci; GA Petersson; H Nakatsuji; M Caricato; X Li; HP Hratchian; AF Izmaylov; J

Bloino; G Zheng; JL Sonnenberg; M Hada; M Ehara; K Toyota; R Fukuda; J Hasegawa; M Ishida; T Nakajim; Y Honda; O Kitao; H Nakai; T Vreven; J A. Montgomery; JrJ E Peralta; F Ogliaro; M Bearpark; JJ Heyd; E Brothers; KN Kudin; VN Staroverov; T Keith; R Kobayashi; J Normand; K Raghavachari; A Rendell; JC Burant; SS Iyengar; J Tomasi; M Cossi; N Rega; JM Millam; M Klene; J E Knox; JB Cross; V Bakken; C Adamo; J Jaramillo; R Gomperts; RE Stratmann; O Yazyev; AJ Austin; R Cammi; C Pomelli; JW Ochterski; R L Martin; K Morokuma; VG Zakrzewski; GA Voth; P Salvador; JJ Dannenberg; S Dapprich; AD Daniels; O Farkas; JB Foresman; JV Ortiz; J Cioslowski; DJ Fox; Gaussian, Inc., Wallingford CT, 2010**.**

[31]Y.F. Shen, J. Tang, Z.H. Nie, Y.D. Wang, Y. Ren and L. Zuo, "Preparation and Application of Magnetic Fe_3O_4 Nanoparticles for Wastewater Purification," Sep. Purif. Technol., vol. 68, 2009,pp. 312–319.

[32]Y. Gao, Y. Masuda, Z. Peng, T. Yonezawa, K. Koumoto, "Room Temperature Deposition of a TiO_2 Thin Film from Aqueous Peroxotitanate Solution," J. Mater. Chem., vol. 13, no. 3, 2003, pp. 608-613.

[33]M. Mahdavi, M.B. Ahmad, M.J. Haron, Y. Gharayebi, K. Shameli and B. Nadi, "Fabrication and Characterization of SiO_2/(3-Aminopropyl) Triethoxysilane-coated Magnetite Nanoparticles for Lead(II) Removal from Aqueous Solution," J. Inorg. Organomet. Polym., vol. 23, 2007, pp. 599–607.

[34]P. Pradhan, J. Giri, G. Samanta, H.D. Sarma, K.P. Mishra, J. Bellare, R. Banerjee and D. Bahadur, "Comparative Evaluation of Heating Ability and Biocompatibility of Different Ferrite-based Magnetic Fluids for Hyperthermia Application," J. Biomed. Mater. Res., vol. 81B, 2006, pp. 12–22.